Urban Textural Analysis from Remote Sensor Data: Lacunarity Measurements Based on the Differential Box Counting Method

Soe W. Myint,[1] Victor Mesev,[2] Nina Lam[3]

[1]Department of Geography, Arizona State University, Tempe, AZ, [2]Department of Geography, Florida State University, Tallahassee, FL, [3]Department of Geography & Anthropology, Louisiana State University, Baton Rouge, LA

Lacunarity is related to the spatial distribution of gap or hole sizes. For low lacunarity, all gap sizes are the same and geometric objects are deemed homogeneous; conversely, for high lacunarity, gap sizes are variable and objects are therefore heterogeneous. Textures that are homogeneous at small scales can be quite heterogeneous at large scales and vice versa, and hence, lacunarity can be considered a scale-dependent measure of heterogeneity or texture. In this article, we use a lacunarity method based on a differential box counting approach to identify urban land-use and land-cover classes from satellite sensor data. Our methodology focuses on two different gliding box methods to compute lacunarity values and demonstrate a mirror extension approach for a local moving window. The extension approach overcomes, or at least minimizes, the boundary problem. The results from our study suggest that the overlapping box approach is more effective than the skipping box approach, but that there is no significant difference between window sizes. Our work represents a contribution to not only advances in textural and spatial metrics as used in remote-sensing pattern interpretation but also for broadening understanding of the computational geometry of nonlinear shape models of which lacunarity is the reciprocal of fractal theory.

Introduction

Despite the new generation of very high spatial resolution sensor data (IKONOS from 1999 and QuickBird from 2001), predicted improvements in classification accuracy of urban land covers (and subsequent inference of urban land use) have yet to materialize substantially (cf. Aplin 2003; Herold, Goldstein, and Clarke 2003). Much of the obstruction to quality information extraction is still due to the traditional limitations of classifying image data representing urban areas: the high

Correspondence: Soe W. Myint, Department of Geography, Arizona State University, 600 E. Orange St., SCOB Bldg, Rm 330, Tempe, AZ 85287-0104
e-mail: Soe.Mynit@asu.edu

spatial arrangement of complex urban features and how to configure multispectral responses from land cover features into organized urban land-use categories (Barr, Barnsley, and Steel 2004). When launched, the desired objective of high spatial resolution sensor data was for increased clarity of terrestrial features, especially urban objects, by reducing per-pixel spectral heterogeneity and thereby improving land cover identification. Clarity is certainly more evident in these finer-scale data than those from preceding sensors, but paradoxically this greater level of detail is also translated into many more unique per-pixel spectral combinations. For example, the residential land-use category can now be defined from much wider spectral variations, representing minute compositional mixtures of urban land covers, such as roads, houses, grasses, trees, bare soil, shrubs, and swimming pools, each conceivably a different residential land-use category. Following on, another limitation for improved information extraction from high spatial resolution sensor data is the reliance on techniques using traditional per-pixel spectral differentiation. To us this seems counterintuitive and we would like to see more neighborhood-related methods, using textural and spatial parameters when dealing with fine-resolution image data. Where traditional spectral approaches are designed to identify homogeneous features regardless of shape, textural and spatial algorithms measure both the variance within and the geometric configuration of whole urban objects, respectively (see Wu et al. 2000; Tullis and Jensen 2003; Herold, Goldstein, and Clarke 2005). As a contribution to the growing literature, we outline an object-based pattern recognition technique that accommodates the concept of lacunarity for characterizing the textural properties of urban land cover (and therefore inferring land use) from high spatial resolution image data. In doing so, we consolidate the utility of geometric models not only for image data but for all discrete and textural spatial representations (Zhao and Stough 2005). Indeed, the ability to characterize the shapes of individual and groups of objects is a rapid area of research in computational geometry and at the heart of the recent developments in object-based models in many geographic information system algorithms (Medda, Nijkamp, and Rietveld 1998; Wentz 2000). Recall that remote sensor data are composed of multispectral pixel vectors that represent geographical objects and their relative configuration. We strongly adhere to the paradigm that geometric patterns, such as lacunarity, are valuable precursors for functional processes; in our application, the texture and spatial orientation of land-cover patterns derived from remote sensor data are both forerunners for analyzing land-use juxtaposition and dynamic urban processes.

Lacunarity approach

The lacunarity of an object is the counterpart of its fractal dimension. Lacunarity methods for urban analysis, and indeed many other applications in geospatial research, have already been reported by a number of researchers (Keller, Chen, and Crownover 1989; Henebry and Kux 1995; Dong 2000a, b; Myint and Lam 2005a). Essentially, lacunarity is related to the spatial distribution of gap or hole sizes. For

low-lacunarity measurements, all gap sizes are the same and geometric objects are deemed homogeneous; conversely, for high-lacunarity gap sizes are variable and objects are therefore heterogeneous. In other words, the variance or texture of gap sizes within the spatial delineation of geometric objects determines the level of lacunarity. Of course, textures that are homogeneous at small scales can be quite heterogeneous at large scales, and vice versa; therefore, lacunarity can be considered a scale-dependent measure of texture (Gefen, Meir, and Aharony 1983). Methods for calculating the lacunarity of objects were first given, in general terms, by Mandelbrot (1983) and were later implemented by various computer algorithms (see Lin and Yang 1986; Voss 1986; Allain and Cloitre 1991; Dong 2000a, b). Work by Myint and Lam (2005b) developed two modified lacunarity algorithms: the binary approach, which was first introduced by Plotnick, Gardner, and O'Neill (1993), and a gray-scale routine, initially devised by Voss (1986) and used to test the effectiveness of lacunarity on high spatial resolution sensor data. This same desire to extract urban objects from fine-scale sensor data also forms the basis of this study, where we examine modifications to a differential box counting algorithm, first formulated by Dong (2000b).

Our study will also introduce two different gliding box approaches. The first uses overlapping boxes, in which the gliding box moves to a pixel next to the previous position (Fig. 1c), and the second uses skipping boxes, in which the gliding box skips the entire coverage of the previous box before moving to the next position (Fig. 1b). As a background, and according to the gliding box algorithm proposed by Allain and Cloitre (1991), $n(M,r)$ can be defined as the number of gliding boxes with radius r and mass M. The probability function $Q(M,r)$ is obtained by dividing $n(M,r)$ by the total number of boxes, so that lacunarity at scale r is defined as

$$\Lambda(r) = \frac{\sum_M M^2 Q(M, r)}{\left[\sum_M MQ(M, r)\right]^2} \tag{1}$$

A cube of size $r \times r \times r$ ($r = 2, 3, 4, \ldots$) is placed over the upper left corner of an image window of size $W \times W$. For each $r \times r$ gliding box, the minimum and maximum pixel values in the gliding box are allowed to fall in box number u and v, respectively. Then, the relative height of the column is

$$n_r(i, j) = v - u - 1 \tag{2}$$

where i and j are image coordinates. Although this calculation gives an accurate height of the column, if the minimum and maximum pixel values fall in the same box, the column becomes a negative one, not a problem if using a positive one. We believe this is adequate as the computed value represents the relative height, so when the $r \times r$ gliding box moves throughout the $W \times W$ image window, the following is possible:

$$M_r = \sum_{i,j} n_r(i, j) \tag{3}$$

(a)

(b)

(c)
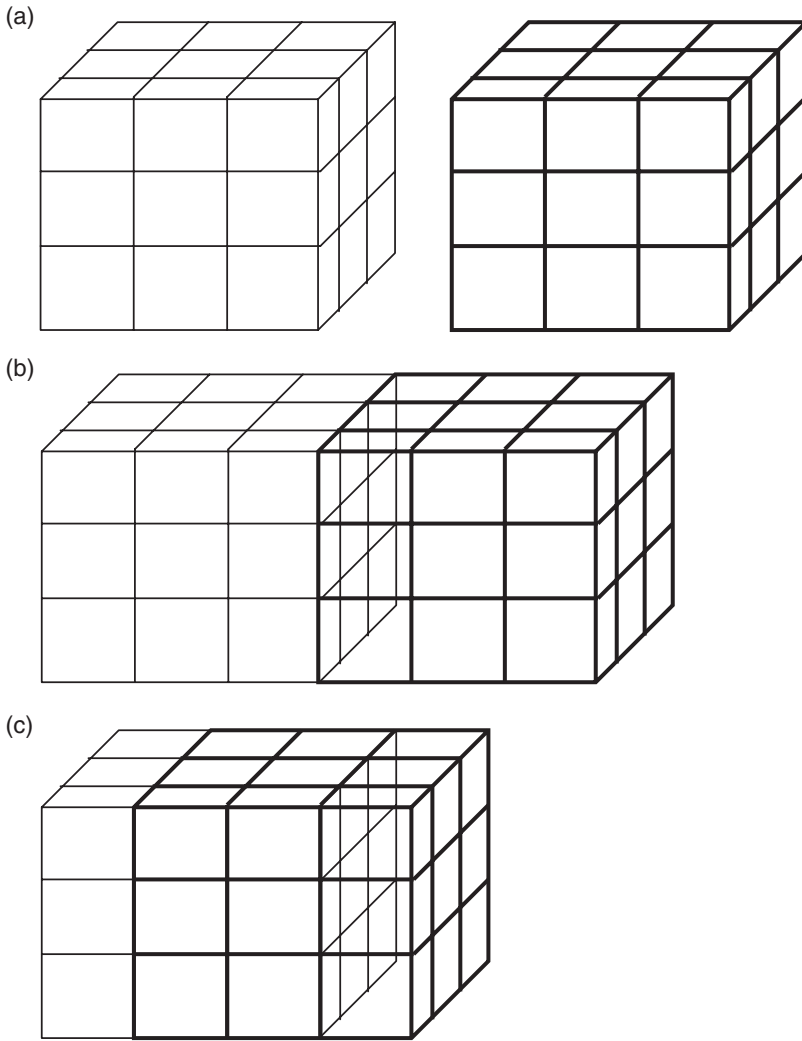
Figure 1. (a) Gliding box with adjacent box. (b) Gliding box and adjacent box in the skipping box algorithm. (c) Gliding box and adjacent box in the overlapping box algorithm.

The mass M in equation (1) is then replaced by M_r to obtain lacunarity $\Lambda(r)$ in the $W \times W$ window (Dong 2000a).

The computations of lacunarity values are given by worked examples in Fig. 2 where the overlapping box method is demonstrated by a 4×4 image or local window (Figs. 2a–e), while a 6×6 image is used to illustrate the skipping box method (Figs. 2f–j). The 3×3 gliding box used in both is the base of the cube box ($3 \times 3 \times 3$ as shown in Fig. 1) and is always an odd number to allow the computed value to be assigned to a central cell. A column with more than one cube box may be required to cover the maximum image intensity values by stacking cube boxes

(a)

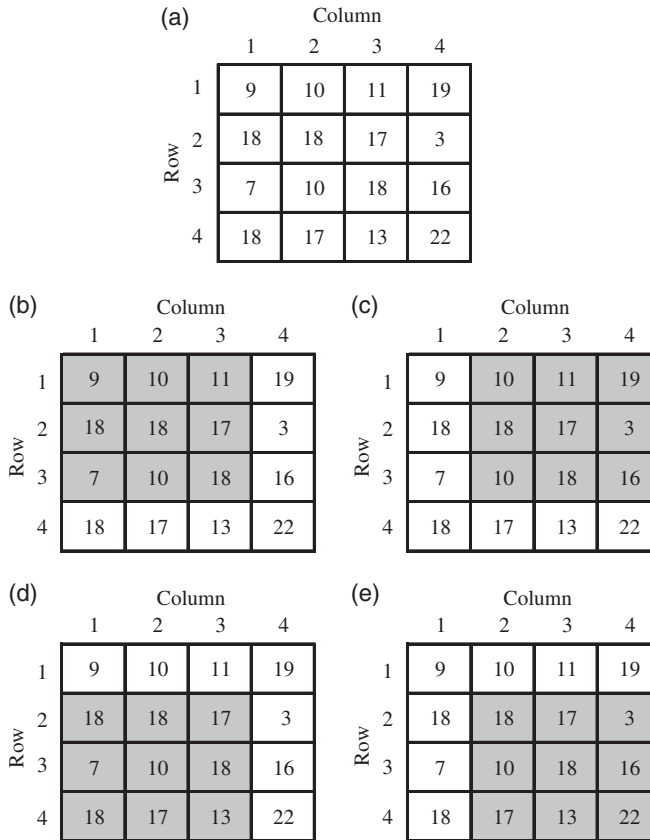|	Column			
	1	2	3	4
1	9	10	11	19
2	18	18	17	3
3	7	10	18	16
4	18	17	13	22

Row

(b)

	Column			
	1	2	3	4
1	9	10	11	19
2	18	18	17	3
3	7	10	18	16
4	18	17	13	22

Row

(c)

	Column			
	1	2	3	4
1	9	10	11	19
2	18	18	17	3
3	7	10	18	16
4	18	17	13	22

Row

(d)

	Column			
	1	2	3	4
1	9	10	11	19
2	18	18	17	3
3	7	10	18	16
4	18	17	13	22

Row

(e)

	Column			
	1	2	3	4
1	9	10	11	19
2	18	18	17	3
3	7	10	18	16
4	18	17	13	22

Row

Figure 2. Worked example to compute lacunarity values for a 4 × 4 image (for an overlapping box) and a 6 × 6 image (for a skipping box) using a 3 × 3 × 3 cube size or a 3 × 3 gliding box (gray shade): (a) 4 × 4 image, (b) first gliding box position within the 4 × 4 image, (c) second gliding box position within the 4 × 4 image, (d) third gliding box position within the 4 × 4 image, (e) fourth gliding box position within the 4 × 4 image, (f) 6 × 6 image, (g) first gliding box position within the 6 × 6 image, (h) second gliding box position within the 6 × 6 image, (i) third gliding box position within the 6 × 6 image, and (j) fourth gliding box position within the 6 × 6 image.

on top of each other. The number of cube boxes required to cover the image intensity surface depends on the pixel values in the 3 × 3 gliding box. Figure 3 illustrates image intensity values in three dimensions, requiring two cube boxes to be stacked on top of each other to cover the entire image intensity column. Intensity values using the example images in Fig. 2 (4 × 4 and 6 × 6 images) are calculated at the first, second, third, and fourth positions of the cube boxes (overlapping and skipping boxes). For example, in Figs. 2b and g the minimum and maximum pixel values are 7 and 18, respectively, at the first position of the gliding box. With a cube box of 3 × 3 × 3, these values fall in box number 3 (value of u) and 6 (value of v),

(f)

	Column					
Row	1	2	3	4	5	6
1	9	10	11	10	11	19
2	18	18	17	18	17	3
3	7	10	18	10	18	16
4	18	18	17	18	17	3
5	7	10	18	10	18	16
6	18	17	13	17	13	22

(g)

	Column					
Row	1	2	3	4	5	6
1	9	10	11	10	11	19
2	18	18	17	18	17	3
3	7	10	18	10	18	16
4	18	18	17	18	17	3
5	7	10	18	10	18	16
6	18	17	13	17	13	22

(h)

	Column					
Row	1	2	3	4	5	6
1	9	10	11	10	11	19
2	18	18	17	18	17	3
3	7	10	18	10	18	16
4	18	18	17	18	17	3
5	7	10	18	10	18	16
6	18	17	13	17	13	22

(i)

	Column					
Row	1	2	3	4	5	6
1	9	10	11	10	11	19
2	18	18	17	18	17	3
3	7	10	18	10	18	16
4	18	18	17	18	17	3
5	7	10	18	10	18	16
6	18	17	13	17	13	22

(j)

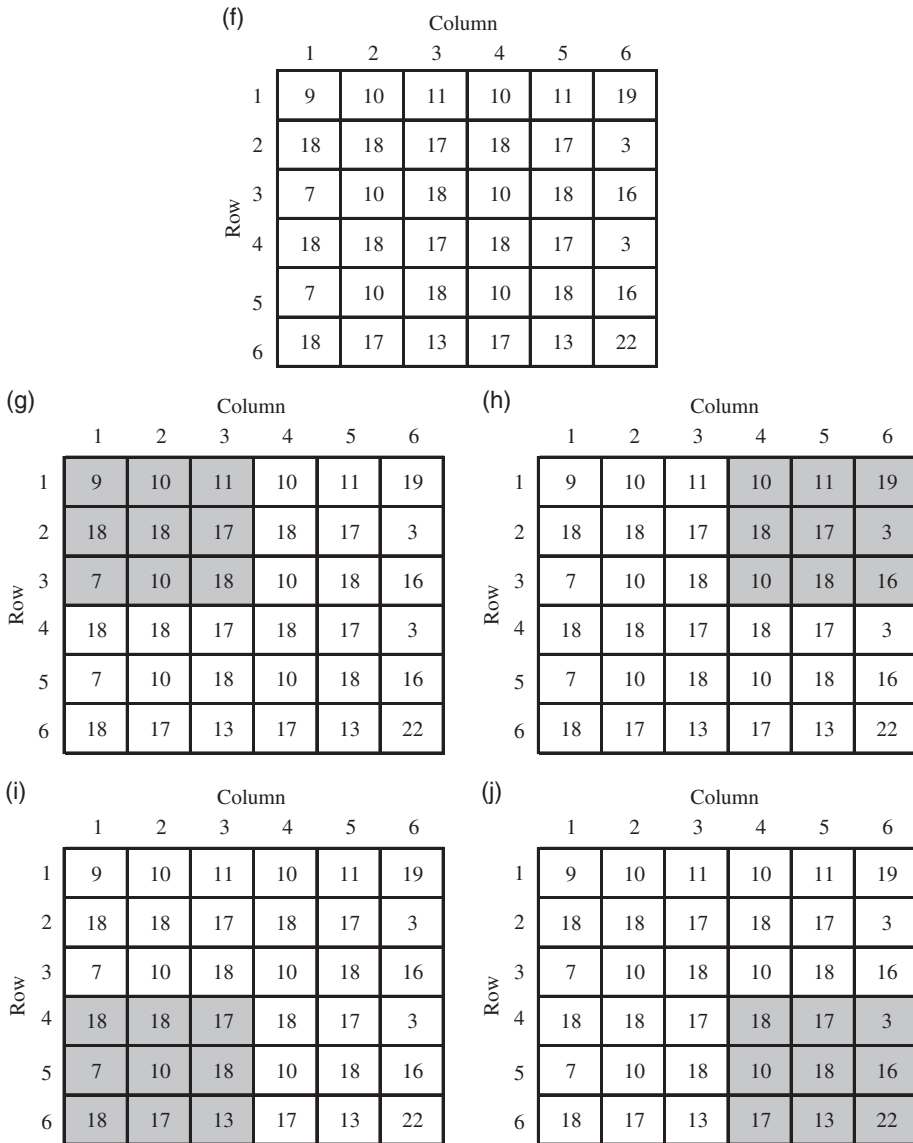|	Column					
Row	1	2	3	4	5	6
1	9	10	11	10	11	19
2	18	18	17	18	17	3
3	7	10	18	10	18	16
4	18	18	17	18	17	3
5	7	10	18	10	18	16
6	18	17	13	17	13	22

Figure 2. Continued.

respectively. The relative height of the column is then $6 - 3 + 1 = 4$ $(u - v + 1)$. In the same way, we can compute the required parameters for all positions of the cube boxes as follows: For the second position of the gliding box, $u = 7$, $v = 1$ (the relative height of the column is $(u - v + 1)$ or $7 - 1 + 1 = 7$). For the third position, $u = 6$; $v = 5$ (the relative height is $6 - 5 + 1 = 2$). For the fourth, $u = 8$, $v = 1$ (the relative height is $8 - 1 + 1 = 8$). Finally, the lacunarity value of the example image is
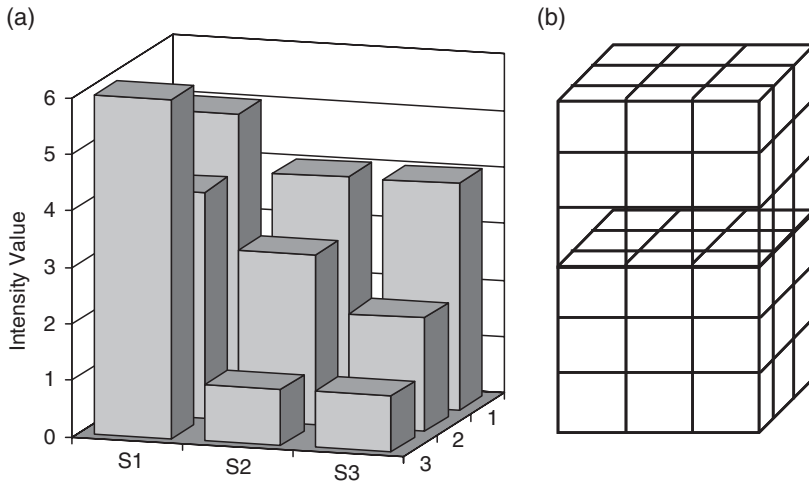
(a)   (b)

Figure 3. (a) Simple image intensity values in three dimensions. (b) Two cube boxes $(3 \times 3 \times 3)$ stacked on top of each other to cover the entire image intensity columns.

calculated as

$$\Lambda(r) = \frac{\sum_M M^2 Q(M, r)}{\left[\sum_M M Q(M, r)\right]^2}$$
$$= [(4 \times 4) \times (1/4)] + [(7 \times 7) \times (1/4)] + [(2 \times 2) \times (1/4)]$$
$$+ [(8 \times 8) \times (1/4)]/[(4/4) + (7/4) + (2/4) + (8/4)]^2 = 1.20635$$

Research design

Data and study area

We applied our technique to an IKONOS sensor image data of 4 m spatial resolution across all four of its channels: blue (0.45–0.52 μm), green (0.52–0.60 μm), red (0.63–0.69 μm), and near infrared (0.76–0.90 μm). The image represents the settlement of Norman, Oklahoma and was captured on March 20, 2000. Only a subset of this IKONOS sensor image (614 × 447 pixels) covering a central portion of the metropolitan area (Fig. 4) was used to identify three land cover/land-use classes: grassland, commercial, and residential—all three capable of being delineated using manual interpretation.

Local window

At the onset, it is important to note that the characteristic scale (Lark 1996) is an important parameter to be considered for effective identification of land covers with different texture appearances. A characteristic scale is the minimum distance between two pixels that completely covers a texture. In our study, anything between

Figure 4. IKONOS image of the study area displaying channel 3 (0.63–0.69 μm) in gray scale.

21 pixels (84 m) and 27 pixels (108 m) was considered large enough to cover textures that represent all of the classes, especially complex residential and commercial land uses derived from the IKONOS multispectral image. Hence, 9 × 9, 15 × 15, 21 × 21, 27 × 27, 33 × 33, and 39 × 39 local window sizes were used to determine the optimum scale with which to identify land-cover classes. From a previous study (Myint and Lam 2005b) that was based on a lacunarity approach designed by Voss (1986), we demonstrated that smaller gliding boxes have more discriminatory power than larger gliding boxes. And as a result, a small 3 × 3 × 3 gliding box is used in this study and is the very basis for the chosen window sizes dimensionalized by a factor of 3. Hypothetically, a window size should be small enough to cover only single land-cover features but large enough to guarantee sufficient spatial/textural information for the characterization of land-cover types. If the local moving window size is $w \times w$, and as the window moves throughout the image the lacunarity value is assigned to the center (at the $[(w+1)/2]$th pixel position), then $(w-1)/2$ pixels are lost from the top, bottom, left, and right side of the image. In that case, a mirror extension of $(w-1)/2$ pixels around the image is necessary before beginning computation. What happens is that the algorithm is designed to extend automatically the image with $(w-1)/2$ pixels all around if the selected window size is w. As such, the size of an extended image is the original image size + (window size − 1). Mirror extension is designed to copy the second-last row or column and add the next-to-last row and column, respectively. Then copy the third-last row and column and add the next-to-the-second-last row and column,
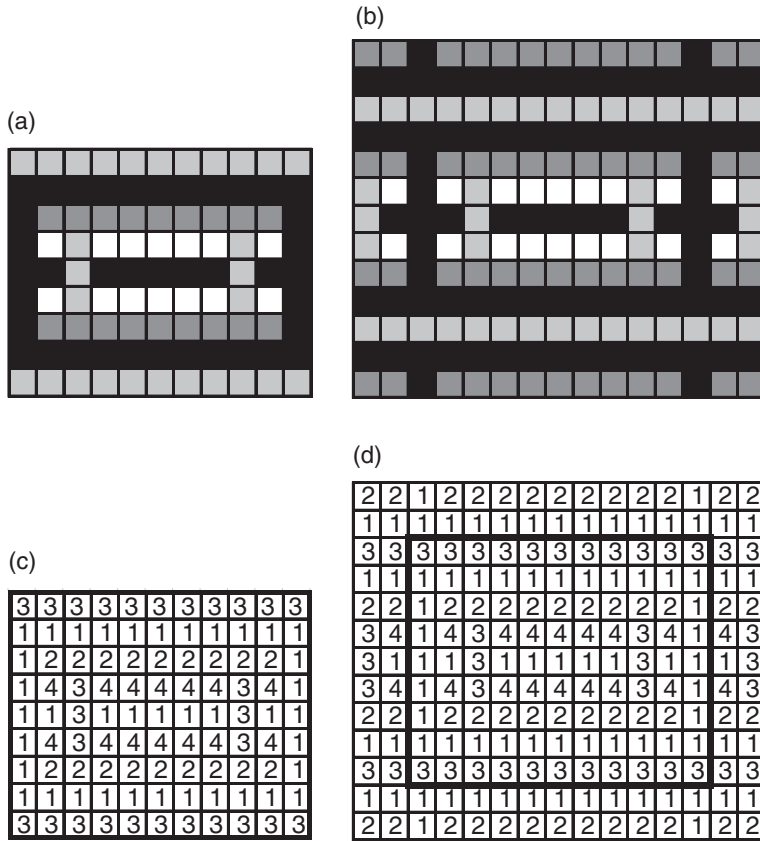
(b)

(a)

(d)

(c)

Figure 5. A hypothetical image in gray scale display and its corresponding brightness values are shown in (a) and (c). The extended images of the above hypothetical images using mirror extension are shown in (b) and (d), respectively.

respectively, and so on depending on the number of rows and columns required for the extension. This mirror extension procedure is demonstrated by a hypothetical image in Fig. 5 and is considered more effective than other widely used methods, including those adding zero, one, last row/column data, or the mean values in the extended areas. Our favored approach is also more accurate than other interpolation methods (e.g., kriging, inverse distance) because it does not alter any values in the original image. By using the mirror extension, we obtain the same mean and standard deviation statistics within the extended area. Moreover, important texture properties, such as characteristic scale, spatial periodicity, and directionality of objects/features, in the extended areas and the original areas in the local window are the same, or at least similar (Lark 1996; Myint 2003). It should also be noted that this extension is performed only during the computational process where the output image has the same number of rows and columns as the original image. An example, illustrating the original image, extended image, local moving window, and
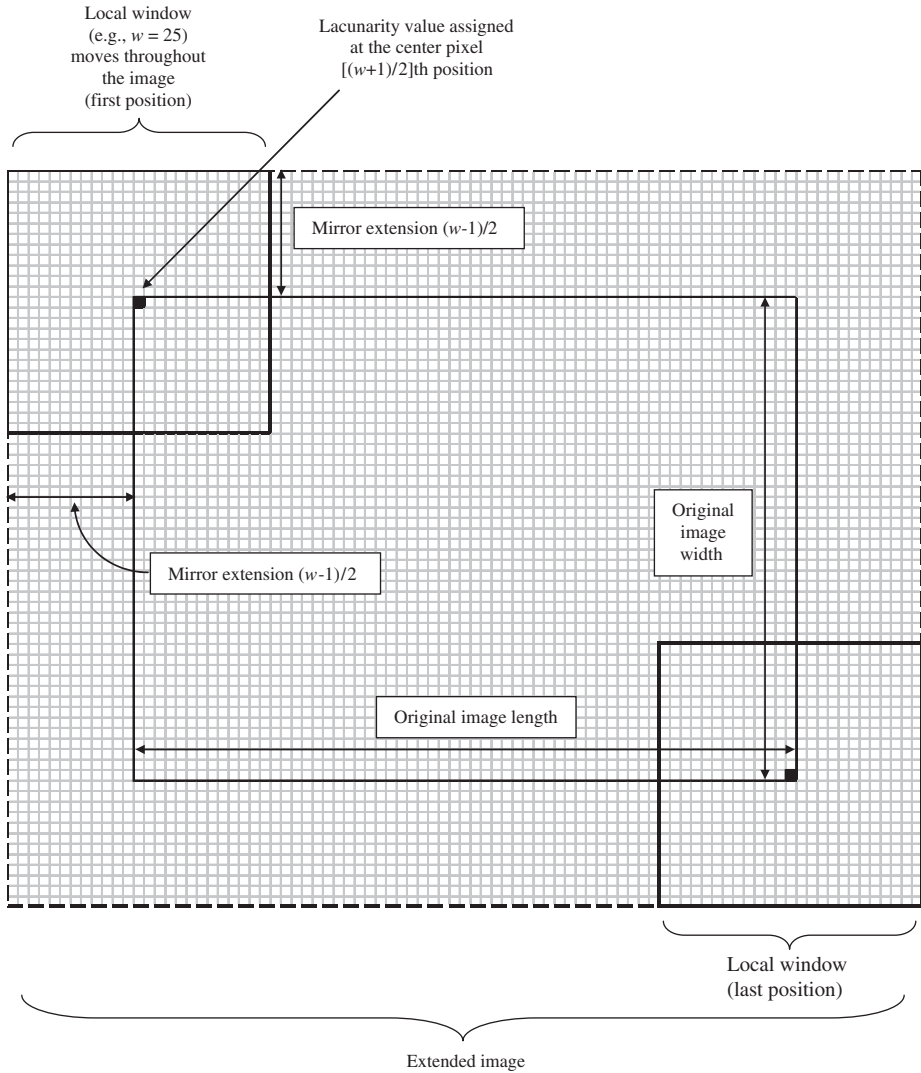
Figure 6. Example showing image extension, moving window and lacunarity value assignment procedure.

assignment of lacunarity value in the local window is presented in Fig. 6. The computed values of the modified lacunarity approach were assigned to the center pixel of the local moving window ($w \times w$) as the window moves through the entire image.

Training samples
With knowledge of the local area and ground checks, training samples were carefully selected to represent the three land-cover/land-use classes: grassland,

Table 1 Descriptive Statistics and Spatial Autocorrelation of the Training Samples

Training sample	Minimum	Maximum	Mean	Standard deviation	Coefficient of variation (%)	Spatial autocorrelation	
						Moran's I	Geary's C
Grassland	185	309	220.48	19.97	9.06	0.49	0.43
Commercial	131	767	423.17	157.05	37.11	0.16	0.83
Residential	135	683	373.44	128.18	34.32	0.09	0.91

commercial, and residential—descriptive statistics of their brightness values are shown in Table 1. It is generally suggested that the standard deviation of training data should be around, or even less than, 10% of the mean coefficient of variation to guarantee homogeneous distributions vital to traditional spectral-based classifiers. Compared with the standard deviation, which is expressed in absolute terms, the coefficient of variation is considered a more appropriate measure for the comparison of data distributions across variables. Again from Table 1, the standard deviation of the commercial and residential land uses is 37.1% and 34.3% of their respective mean values. At this stage, it is important to remember that groups of adjacent pixels generally exhibit positive autocorrelation, or at least display a high probability of having similar digital numbers (cf. Gong and Howarth 1992; Emerson, Lam, and Quattrochi 1999; Warner, Steinmaus, and Foote 1999; Jensen 2004). In our calculations, the grassland (Moran's $I = 0.49$; Geary's $C = 0.43$) sample exhibited a positive autocorrelation, whereas the commercial (Moran's $I = 0.16$; Geary's $C = 0.83$) and residential (Moran's $I = 0.09$; Geary's $C = 0.91$) samples displayed random spatial arrangements with no patterns of clustering or homogeneity (Table 1).

Band combinations and classifications

Finally, lacunarity algorithms, based on both skipping and overlapping boxes, were applied to transform bands 2, 3, and 4 of the IKONOS image. In addition, a number of layer stacks involving both lacunarity-transformed bands and original bands were generated in the following combinations:

- three original bands,
- three lacunarity-transformed bands,
- combination of three original bands and three lacunarity-transformed bands,
- combination of three original and one lacunarity-transformed band, and
- combination of two original bands and two lacunarity-transformed bands.

All window sizes were applied to stacks of three original bands and three lacunarity-transformed bands, as well as the combination of three original bands and one lacunarity-transformed band. Regarding the three separate lacunarity-transformed bands, only the 27×27 window was used, primarily to observe whether

satisfactory accuracy levels were attained without the original bands. In the case of the combination of the three original bands and one lacunarity-transformed band, the lacunarity-transformed band 3 was used to test whether one lacunarity-transformed band could improve the accuracy of the three original bands. Experiments were conducted with all window sizes using lacunarity-transformed band 3, as well as testing lacunarity-transformed band 4 with the original bands using the 27×27 window for significant differences between lacunarity-transformed band 3 and lacunarity-transformed band 4. In the case of the combination of two original bands and two lacunarity-transformed bands, band 3 and band 4 were tested using the 27×27 window. All code for the modified lacunarity approaches was written in the C++ programming language.

Reference map for error matrix

When examining the effectiveness of different classification algorithms, "wall-to-wall" comparisons were used by checking every pixel in the image. The selected area covered 274,458 pixels (447×614) representing all three urban classes: grassland, commercial, and residential. Reference classes were collected by manual interpretation, using sound local area knowledge and a thorough ground survey, and then digitally delineated with negligible positional error.

Results and discussion

Overall accuracies produced by the combination of three original bands and three lacunarity-transformed bands using the overlapping box algorithm based on the 9×9, 15×15, 21×21, 27×27, 33×33, and 39×39 window sizes were 59.36%, 61.72%, 61.86%, 61.01%, 59.94%, and 61.65%, respectively. They demonstrate that overall accuracy increases slightly with expanding window sizes, despite a slight decline when using the 33×33 window (Table 2), and it is fairly reasonable to suggest that the 15×15 and 21×21 window sizes are effective for this analysis. However, overall accuracies produced by the combination of three original bands and three lacunarity-transformed bands using the skipping box algorithm based on the 9×9, 15×15, 21×21, 27×27, 33×33, and 39×39 window sizes were 58.31%, 59.29%, 57.40%, 56.41%, 56.92%, and 58.31%, respectively (Table 3). Different window sizes produced inconsistent overall accuracies, and hence it is difficult to determine the optimal window size. In comparison, the overlapping box algorithm outperforms the skipping box algorithm, and because the overall accuracy of the original bands is 58.38% (Table 4), it can be concluded that lacunarity using the overlapping box algorithm improved the classification accuracy of the original bands. However, we feel that accuracy was not significantly improved.

Overall accuracies produced by the combination of three original bands and one lacunarity-transformed band (band 3) using the overlapping box algorithm based on the 9×9, 15×15, 21×21, 27×27, 33×33, and 39×39 window sizes were 58.49%, 60.74%, 60.94%, 60.43%, 60.29%, and 61.35%, respectively

Table 2 Overall Accuracies Produced by the Combination of Three Original Bands and Three Lacunarity-Transformed Bands for Overlapping Box Algorithm Using (a) 9×9, (b) 15×15, (c) 21×21, (d) 27×27, (e) 33×33, and (f) 39×39 Window Sizes

	Reference data			Total points	Accuracy	
	G	C	R		Producer's accuracy (%)	User's accuracy (%)
(a) 9×9 window						
G	27,180	1141	8663	36,984	42	73
C	2724	57,878	38,761	99,363	68	58
R	34,615	25,633	77,863	138,111	62	56
Total points	64,519	84,652	125,287	274,458	Overall accuracy = 59.36	$\kappa = 0.35$
(b) 15×15 window						
G	27,693	497	3097	31,287	43	89
C	4028	57,512	38,005	99,545	68	58
R	32,798	26,643	84,185	143,626	67	59
Total points	64,519	84,652	125,287	274,458	Overall accuracy = 61.72	$\kappa = 0.38$
(c) 21×21 window						
G	24,364	192	522	25,078	38	97
C	3805	51,232	30,569	85,606	61	60
R	36,350	33,228	94,196	163,774	75	58
Total points	64,519	84,652	125,287	274,458	Overall accuracy = 61.86	$\kappa = 0.37$
(d) 27×27 window						
G	18,409	2	56	18,467	29	100
C	2874	45,424	21,618	69,916	54	65
R	43,236	39,226	103,613	186,075	83	56
Total points	64,519	84,652	125,287	274,458	Overall accuracy = 61.01	$\kappa = 0.35$
(e) 33×33 window						
G	17,314	0	0	17,314	27	100
C	2956	39,776	17,855	60,587	47	66
R	44,249	44,876	107,432	196,557	86	55
Total points	64,519	84,652	125,287	274,458	Overall accuracy = 59.94	$\kappa = 0.32$
(f) 39×39 window						
G	20,927	0	4	20,931	32	100
C	4286	39,939	16,958	61,183	47	65
R	39,306	44,713	108,325	192,344	86	56
Total points	64,519	84,652	125,287	274,458	Overall accuracy = 61.65	$\kappa = 0.35$

G, grasslands; C, commercial; R, residential.

(Table 5). From this, we can deduce that there is only a slight difference between adding the one lacunarity-transformed band (band 3) to the original bands and adding three lacunarity-transformed bands to the original bands. However, it was

Table 3 Overall Accuracies Produced by the Combination of Three Original Bands and Three Lacunarity-Transformed Bands for Skipping Box Algorithm Using (a) 9 × 9, (b) 15 × 15, (c) 21 × 21, (d) 27 × 27, (e) 33 × 33, and (f) 39 × 39 Window Sizes

	Reference Data			Total points	Accuracy	
	G	C	R		Producer's accuracy (%)	User's accuracy (%)
(a) 9 × 9 window						
G	26,390	673	4057	31,120	41	85
C	2035	51,120	35,964	89,119	60	57
R	36,094	32,859	85,266	154,219	68	55
Total points	64,519	84,652	125,287	274,458	Overall accuracy = 59.31	κ = 0.34
(b) 15 × 15 window						
G	20,886	173	500	21,559	32	97
C	1603	49,967	32,910	84,480	59	59
R	42,030	34,512	91,877	168,419	73	55
Total points	64,519	84,652	125,287	274,458	Overall accuracy = 59.29	κ = 0.33
(c) 21 × 21 window						
G	16,213	9	22	16,244	25	100
C	1274	41,254	25,197	67,725	49	61
R	47,032	43,389	100,068	190,489	80	53
Total points	64,519	84,652	125,287	274,458	Overall accuracy = 57.40	κ = 0.28
(d) 27 × 27 window						
G	13,329	0	1	13,330	21	100
C	1286	35,450	19,240	55,976	42	63
R	49,904	49,202	106,046	205,152	85	52
Total points	64,519	84,652	125,287	274,458	Overall accuracy = 56.41	κ = 0.25
(e) 33 × 33 window						
G	14,427	0	0	14,427	22	100
C	1468	33,344	16,836	51,648	39	65
R	48,624	51,308	108,451	208,383	87	52
Total points	64,519	84,652	125,287	274,458	Overall accuracy = 56.92	κ = 0.26
(f) 39 × 39 window						
G	18,974	0	4	18,978	29	100
C	2127	32,351	16,577	51,055	38	63
R	43,418	52,301	108,706	204,425	87	53
Total points	64,519	84,652	125,287	274,458	Overall accuracy = 58.31	κ = 0.29

G, grasslands; C, commercial; R, residential.

also found that the combination of three original bands and three lacunarity-transformed bands produced higher accuracies. Overall accuracies generated by the combination of three original bands and one lacunarity-transformed band (band 4)

Table 4 Overall Accuracies Produced by (a) Three Original Bands, (b) Three Original Bands and One Lacunarity-Transformed Band (i.e., Band 4) Using the Overlapping Box Algorithm for 15 × 15 Window Size, (c) Three Original Bands and One Lacunarity-Transformed Band (i.e., Band 4) Using the Overlapping Box Algorithm for 27 × 27 Window Size, (d) Lacunarity-Transformed Bands Alone, (e) Two Original Bands (i.e., Bands 3 and 4) and Two Lacunarity-Transformed Bands (i.e., Bands 3 and 4) for the Overlapping Box Algorithm Using 27 × 27 Local Window, and (f) the Expert System Approach

	Reference Data			Total points	Accuracy	
	G	C	R		Producer's accuracy (%)	User's accuracy (%)
(a) 3 original bands						
G	25,865	1003	8433	35,301	40	73
C	2876	60,208	42,702	105,786	71	57
R	35,778	23,441	74,152	133,371	59	56
Total points	64,519	84,652	125,287	274,458	Overall accuracy = 58.38	κ = 0.34
(b) 15 × 15 window, 3 original bands and lacunarity-transformed band 4						
G	26,550	1426	10,947	38,923	41	68
C	2634	59,464	40,782	102,880	70	58
R	35,335	23,762	73,558	132,655	59	55
Total points	64,519	84,652	125,287	274,458	Overall accuracy = 58.14	κ = 0.34
(c) 27 × 27 window, 3 original bands and lacunarity-transformed band 4						
G	21,449	641	5883	27,973	33	77
C	2811	58,727	37,666	99,204	69	59
R	40,259	25,284	81,738	147,281	65	55
Total points	64,519	84,652	125,287	274,458	Overall accuracy = 58.99	κ = 0.34
(d) 27 × 27 window, Lacunarity-transformed bands alone						
G	26,374	1444	11,232	39,050	41	68
C	2670	59,788	41,569	104,027	71	57
R	35,475	23,420	72,486	131,381	58	55
Total points	64,519	84,652	125,287	274,458	Overall accuracy = 57.80	κ = 0.33
(e) 27 × 27 window, Original bands 3 and 4 and lacunarity-transformed bands 3 and 4						
G	18,002	17	94	18,113	28	99
C	1560	45,299	20,651	67,510	54	67
R	44,957	39,336	104,542	188,835	83	55

G, grasslands; C, commercial; R, residential.

using the overlapping box algorithm for the 15 × 15 and 27 × 27 window sizes (58.14% and 58.99%, respectively) were lower (Table 4) than the combination with lacunarity-transformed band 3. Overall accuracies produced by the combination of three original bands and one lacunarity-transformed band (band 3) for the skipping box algorithm using the 9 × 9, 15 × 15, 21 × 21, 27 × 27, 33 × 33, and 39 × 39 window sizes were 58.87%, 60.07%, 58.60%, 57.37%, 56.93%, and 57.69%,

Table 5 Overall Accuracies Produced by the Combination of Three Original Bands and One Lacunarity-Transformed Band (i.e., Band 3) for the Overlapping Box Algorithm Using 9 × 9, 15 × 15, 21 × 21, 27 × 27, 33 × 33, and 39 × 39 Window Sizes

	Reference Data			Total points	Accuracy	
	G	C	R		Producer's accuracy (%)	User's accuracy (%)
(a) 9 × 9 window						
G	26,864	1319	10,193	38,376	42	70
C	2700	59,249	40,691	102,640	70	58
R	34,955	24,084	74,403	133,442	59	56
Total points	64,519	84,652	125,287	274,458	Overall accuracy = 58.48	κ = 0.34
(b) 15 × 15 window						
G	26,994	638	5202	32,834	42	82
C	3107	59,045	39,431	101,583	70	58
R	34,418	24,969	80,654	140,041	64	58
Total points	64,519	84,652	125,287	274,458	Overall accuracy = 60.74	κ = 0.37
(c) 21 × 21 window						
G	23,449	214	706	24,369	36	96
C	1967	48,587	29,370	79,924	57	61
R	39,103	35,851	95,211	170,165	76	56
Total points	64,519	84,652	125,287	274,458	Overall accuracy = 60.94	κ = 0.36
(d) 27 × 27 window						
G	17,453	6	55	17,514	27	100
C	1087	42,165	19,000	62,252	50	68
R	45,979	42,481	106,232	194,692	85	55
Total points	64,519	84,652	125,287	274,458	Overall accuracy = 60.43	κ = 0.33
(e) 33 × 33 window						
G	15,980	0	0	15,980	25	100
C	1230	39,977	15,768	56,975	47	70
R	47,309	44,675	109,519	201,503	87	54
Total points	64,519	84,652	125,287	274,458	Overall accuracy = 60.29	κ = 0.32
(f) 39 × 39 window						
G	20,085	0	0	20,085	31	100
C	1639	38,760	15,763	56,162	46	69
R	42,795	45,892	109,524	198,211	87	55
Total points	64,519	84,652	125,287	274,458	Overall accuracy = 61.35	κ = 0.34

G, grasslands; C, commercial; R, residential.

respectively (Table 6). The results show that there is no difference between adding three lacunarity-transformed bands to the original bands or adding one lacunarity-transformed band (band 3) to the original bands. This may be mainly because the

Table 6 Overall Accuracies Produced by the Combination of Three Original Bands and One Lacunarity-Transformed Band (i.e., Band 3) for the Skipping Box Algorithm Using 9 × 9, 15 × 15, 21 × 21, 27 × 27, 33 × 33, and 39 × 39 Window Sizes

	Reference data			Total points	Accuracy	
	G	C	R		Producer's accuracy (%)	User's accuracy (%)
(a) 9 × 9 window						
G	26,892	1042	7907	35,841	42%	75
C	2343	56,656	39,357	98,356	67	58
R	35,284	26,954	78,023	140,261	62	56
Total points	64,519	84,652	125,287	274,458	Overall accuracy = 58.87	κ = 0.34
(b) 15 × 15 window						
G	22,239	225	1301	23,765	34	94
C	2193	57,198	38,560	97,951	68	58
R	40,087	27,229	85,426	152,742	68	56
Total points	64,519	84,652	125,287	274,458	Overall accuracy = 60.07	κ = 0.35
(c) 21 × 21 window						
G	18,302	26	180	18,508	28	99
C	1703	49,465	32,039	83,207	58	59
R	44,514	35,161	93,068	172,743	74	54
Total points	64,519	84,652	125,287	274,458	Overall accuracy = 59.60	κ = 0.31
(d) 27 × 27 window						
G	15,747	3	36	15,786	24	100
C	1459	41,909	25,451	68,819	50	61
R	47,313	42,740	99,800	189,853	80	53
Total points	64,519	84,652	125,287	274,458	Overall accuracy = 57.37	κ = 0.28
(e) 33 × 33 window						
G	15,299	0	14	15,313	24	100
C	1531	37,780	22,100	61,411	45	62
R	47,689	46,872	103,173	197,734	82	52
Total points	64,519	84,652	125,287	274,458	Overall accuracy = 56.93	κ = 0.27
(f) 39 × 39 window						
G	17,942	0	18	17,960	28	100
C	1716	35,345	20,226	57,287	42	62
R	44,861	49,307	105,043	199,211	84	53
Total points	64,519	84,652	125,287	274,458	Overall accuracy = 57.69	κ = 0.28

G, grasslands; C, commercial; R, residential.

skipping box algorithm is not particularly effective in identifying texture features from image data. As mentioned earlier, we also tested the lacunarity-transformed bands generated by the overlapping box approach, individually. These texture

bands on their own gave slightly lower accuracy (57.80%) than the individual original bands (Table 4), which tends to imply that spatial information alone may not be effective in identifying land-use/land-cover classes (an area we intend to research further). We also examined the combination of two original bands (bands 3 and 4) and two lacunarity-transformed bands (again bands 3 and 4) using the overlapping box algorithm based on the 27 × 27 local window. The results from this approach produced an accuracy level (Table 4) as high as the combination of three original bands and three lacunarity-transformed bands. This is probably because IKONOS bands 2 and 3 are visible bands and therefore highly correlated.

Conclusions

Urban remote sensing is currently experiencing a paradigm shift away from spectral-only classification and toward the identification of urban objects using spatial metrics and neighborhood-based pattern recognition. Most of the conceptual restructuring is underscored by the availability of very high spatial resolution imagery, but also by the practical necessity of generating base maps of urban land use. Our work reported in this article is a contribution to research on spatial and textural identification of urban objects. We explored the utility of lacunarity to measure urban heterogeneity where results suggest that the overlapping box approach is more effective than the skipping box alternative. We documented that there is no significant difference between window sizes, except for the case of the 9 × 9 window, and it might be reasonable to conclude that the 15 × 15, 21 × 21, and 27 × 27 windows are the most effective sizes in our study. It was also found that the combination of two original bands (bands 3 and 4) and two lacunarity-transformed bands (bands 3 and 4) is as accurate as the combination of three original bands and three lacunarity-transformed bands. The combination of three original bands and three lacunarity-transformed bands is only a slight improvement on the combination of three original bands and one lacunarity-transformed band (band 3). However, what is certain is that the original bands alone or the purely lacunarity-transformed bands are not effective for this type of land-use and land-cover mapping.

As a footnote, although variable, our results are very much in line with other documented work on textural and spatial characterization of high spatial resolution sensor data of urban land cover. It seems metrics, be they indices of dispersion, contagion, fractal, or lacunarity, are highly sensitive to the initial image segmentation, and inextricably affected by site, time, and scene. Another reason for small and variable improvements in urban representation is the conceptual gulf between the computational limitations of the discretized remote sensor data model and the heterogeneous and dynamic nature of the urban landscape. Such a gulf may prove difficult to bridge immediately with either spectral or textural/spatial indices, and a more integrative approach may ultimately be more appropriate. However, for now

our work on lacunarity demonstrates another contribution to the potential for spatial metrics to characterize the increasingly finer spatial resolution of remote sensor data. We hold firm to our belief that highly detailed, spatially heterogeneous urban land cover can be measured by algorithms that are equally sensitive to geometric fluctuations.

Acknowledgement

References

Allain, C., and M. Cloitre. (1991). ''Characterizing the Lacunarity of Random and Deterministic Fractal Sets.'' *Physics Review A* 44, 3552–58.

Aplin, P. (2003). ''Comparison of Simulated IKONOS and SPOT HRV Imagery for Classifying Urban Areas.'' In *Remotely Sensed Cities*, 23–45, edited by V. Mesev. London: Taylor & Francis.

Barr, S. L., M. J. Barnsley, and A. Steel. (2004). ''On the Separability of Urban Land-Use Categories in Fine Spatial Scale Land-Cover Data Using Structural Pattern Recognition.'' *Environment and Planning B* 31, 397–418.

Dong, P. (2000a). ''Lacunarity for Spatial Heterogeneity Measurement in GIS.'' *Geographic Information Sciences* 6, 20–26.

Dong, P. (2000b). ''Test of a New Lacunarity Estimation Method for Image Texture Analysis.'' *International Journal of Remote Sensing* 21, 3369–73.

Emerson, C. W., N. S. N. Lam, and D. A. Quattrochi. (1999). ''Multi-Scale Fractal Analysis of Image Texture and Pattern.'' *Photogrammetric Engineering and Remote Sensing* 65, 51–61.

Gefen, Y., Y. Meir, and A. Aharony. (1983). ''Geometric Implementation of Hypercubic Lattices with Non-Integer Dimensionality by Use of Low Lacunarity Fractal Lattices.'' *Physical Review Letters* 50, 145–48.

Gong, P., and P. J. Howarth. (1992). ''Frequency Based Contextual Classification and Gray Level Vector Reduction for Land Use Identification.'' *Photogrammetric Engineering and Remote Sensing* 58, 423–37.

Henebry, G. M., and H. J. H. Kux. (1995). ''Lacunarity as a Texture Measure for SAR Imagery.'' *International Journal of Remote Sensing* 16, 565–71.

Herold, M., N. C. Goldstein, and K. C. Clarke. (2003). ''The Spatiotemporal Form of Urban Growth.'' *Remote Sensing of Environment* 86, 286–302.

Herold, M., H. Couclelis, and K. C. Clarke. (2005). ''The Role of Spatial Metrics in the Analysis and Modeling of Urban Land Use Change.'' *Environment and Planning A* 34, 369–99.

Jensen, J. R. (2004). *Introductory Digital Image Processing, A Remote Sensing Perspectives.* Upper Saddle River, NJ: Prentice-Hall.

Keller, J. M., S. Chen, and R. M. Crownover. (1989). ''Texture Description and Segmentation Through Fractal Geometry.'' *Computer Vision, Graphics, and Image Processing* 45, 150–66.

Lark, R. M. (1996). ''Geostatistical Description of Texture on an Aerial Photograph for Discriminating Classes of Land Cover.'' *International Journal of Remote Sensing* 17, 2115–33.

Lin, B., and Z. R. Yang. (1986). ''A Suggested Lacunarity Expression for Sierpinski Carpets.'' *Journal Physics A: Mathematical and General* 19, L49–52.

Mandelbrot, B. B. (1983). *The Fractal Geometry of Nature*. New York: Freeman and Co.

Medda, F. P., P. Nijkamp, and P. Rietveld. (1998). ''Recognition and Classification of Urban Shapes.'' *Geographical Analysis* 30, 304–14.

Myint, S. W. (2003). ''The Use of Wavelets for Feature Extraction of Cities in Satellite Images.'' In *Remotely Sensed Cities*, 109–34, edited by V. Mesev. London: Taylor & Francis.

Myint, S. W., and N. S. N. Lam. (2005a). ''A Study of Lacunarity-Based Texture Analysis Approaches to Improve Urban Image Classification.'' *Computers, Environment, and Urban Systems* 29, 501–23.

Myint, S. W., and N. S. N. Lam. (2005b). ''Examining Lacunarity Approaches in Comparison with Fractal and Spatial Autocorrelation Techniques for Urban Mapping.'' *Photogrammetric Engineering and Remote Sensing* 71, 927–37.

Plotnick, R. E., R. H. Gardner, and R. V. O'Neill. (1993). ''Lacunarity Indices as Measures of Landscape Texture.'' *Landscape Ecology* 8, 201–11.

Tullis, J. A., and J. R. Jensen. (2003). ''Expert System House Detection in High Spatial Resolution Imagery Using Size, Shape, and Context.'' *Geocarto International* 18, 5–15.

Voss, R. (1986). ''Random Fractals: Characterization and Measurement.'' In *Scaling Phenomena in Disordered Systems*, 37–48, edited by R. Pynn and A. Skjeltorp. New York: Plenum.

Warner, T. A., K. Steinmaus, and H. Foote. (1999). ''An Evaluation of Spatial Autocorrelation Feature Selection.'' *International Journal of Remote Sensing* 20, 1601–16.

Wentz, E. A. (2000). ''Shape Definition for Geographic Applications Based on Edge, Elongation, and Perforation.'' *Geographical Analysis* 32, 204–13.

Wu, J., E. J. Jelinski, M. Luck, and M. P. T. Tueller. (2000). ''Multiscale Analysis of Landscape Heterogeneity: Scale Variance and Pattern Metric.'' *Geographic Information Sciences* 6, 6–16.

Zhao, Z., and R. R. Stough. (2005). ''Measuring Similarity Among Various Shapes Based on Geometric Matching.'' *Geographical Analysis* 37, 410–22.